Protein Science (2000), *9*:2225–2231. Cambridge University Press. Printed in the USA.

Phosphoryl transfer by a concerted reaction mechanism in UMP/CMP-kinase

MICHAEL C. HUTTER AND VOLKHARD HELMS

Max-Planck-Institute of Biophysics, Kennedyallee 70, D-60596 Frankfurt, Germany

(RECEIVED April 19, 2000; FINAL REVISION August 21, 2000; ACCEPTED August 24, 2000)

Abstract

The reaction mechanism of phosphoryl transfer catalyzed by UMP/CMP-kinase from *Dictyostelium discoideum* was investigated by semiempirical AM1 molecular orbital computations of an active site model system derived from crystal structures that contain a transition state analog or a bisubstrate inhibitor. The computational results suggest that the nucleoside monophosphate must be protonated for the forward reaction while it is unprotonated in the presence of aluminium fluoride, a popular transition state analog for phosphoryl transfer reactions. Furthermore, a compactification of the active site model system during the reaction and for the corresponding complex containing AlF_3 was observed. For the active site residues that are part of the LID domain, conformational flexibility during the reaction proved to be crucial. On the basis of the calculations, a concerted phosphoryl transfer mechanism is suggested that involves the synchronous shift of a proton from the monophosphate to the transferred PO_3-group. The proposed mechanism is thus analogous to the phosphoryl transfer mechanism in cAMP-dependent protein kinase that phosphorylates the hydroxyl groups of serine residues.

Keywords: nucleoside monophosphate kinase; phosphoryl transfer; reaction mechanism; semiempirical molecular orbital calculation; transition state analog; UMP/CMP-kinase

The range of phosphoryl transfer reactions in biological systems comprises processes such as energy and signal transduction, activation of metabolites, and cell growth (Bossemeyer, 1995; Mildvan, 1997). In the latter case, the activation of nucleosides to nucleoside triphosphates to be used in DNA and RNA synthesis is mediated by monophosphate kinases (NMP-kinases) that formally transfer a phosphate group from one nucleoside to another (Yan & Tsai, 1999).

Common to all proteins of the adenylate kinase family are three structural subunits termed CORE, NMPbind, and LID domain (Vonrhein et al., 1995). The rigid CORE region includes the central parallel β-sheet and the P-loop that plays an important role in binding the triphosphate moiety of ATP. Likewise, the nucleoside monophosphate is bound in the NMPbind region. The catalytic LID domain was shown to close over the negatively charged phosphate groups of the two ligated nucleosides donating highly conserved arginines. Compared to other variants of NMP kinases homologous to adenylate kinase, this region is rather short in UMP/CMP kinase from *Dictyostelium discoideum* (10 residues). The flexibility of the NMPbind and the LID domains is indicated by their high *B*-factors found in crystallographic studies (Scheffzek et al., 1996; Schlichting & Reinstein, 1997) and by a structural comparison among NMP kinases (Vonrhein et al., 1995).

For UMP/CMP-kinase from *D. discoideum* that catalyzes the reversible phosphoryl transfer between ATP and UMP or CMP (Yan & Tsai, 1999), a significant background of experimental work has been established, especially structural studies by X-ray crystallography (Scheffzek et al., 1996; Schlichting & Reinstein, 1997, 1999).

Nevertheless, the actual reaction mechanism of phosphoryl transfer in dinucleoside kinases is still not fully understood; particularly the discussion whether the mechanism is associative or dissociative remains controversial (Mildvan, 1997; Schlichting & Reinstein, 1997; Yan & Tsai, 1999). With PO_3 as the transferred group, the following arguments can be used to assign the mechanism within two extremes (Admiraal & Herschlag, 1995): In a fully dissociative mechanism, the γ-phosphate is cleaved from ATP to form a monoanionic metaphosphate in the transition state that is then transferred to P_α of the mononucleoside. This mechanism is true if the distances from the phosphorus atom in the transition state to the oxygen atoms on the β-phosphate and on the α-phosphate are large enough ($\geq$3.3 Å, respectively) (Mildvan, 1997). In contrast, a fully associative mechanism involves a highly negatively

Reprint requests to: Volkhard Helms, Max-Planck-Institute of Biophysics, Kennedyallee 70, Frankfurt, D-60596 Germany; e-mail: vhelms@mpibp-frankfurt.mpg.de.

Abbreviations: AM1, Austin Model 1; ADP, adenosine diphosphate; ATP, adenosine triphosphate; cAPK, cAMP-dependent protein kinase; CMP, cytosine monophosphate; NMP-kinase, nucleoside monophosphate kinase; UMP, uridine monophosphate; UMP/CMP-kinase, uridinemonophosphate-cytosinemonophosphate kinase.

charged metaphosphate with a pentacoordinated phosphorus. The distances between phosphorus and the apical oxygens should be around 1.7 Å corresponding to covalent single P–O bonds. While direct experimental observation of the reaction has not been reported quite some effort has been spent on finding suitable inhibitors or transition state analogs that mimic the corresponding states of the reaction (Scheffzek et al., 1996; Schlichting & Reinstein, 1997, 1999). Quantum chemical methods, on the other hand, are ideally suited to determine structures of transition states: These are saddle points along a reaction coordinate and therefore well defined.

Up to only a few years ago, theoreticians have focused on a few enzymatic model systems such as carbonic anhydrase (Merz et al., 1989; Åqvist et al., 1993). Recent years, however, have seen an enormous increase of theoretical studies of enzymatic reactions, either using purely quantum mechanical systems, or increasingly popular, combined quantum mechanical /molecular mechanical approaches (Gao, 1995). With the focus on enzymatic phosphoryl transfer, Schweins et al. (1994, 1996) have studied ras p21 with the empirical valence bond approach. On the other hand, quantum chemical ab initio studies of phosphoryl transfer have so-far focused, with quite some success, on the hydrolysis of methyl phosphate in solution. Here, a dissociative mechanism is favored over an associative mechanism by more than 10 kcal mol^{-1} (Hu & Brinck, 1999) in agreement with recent experimental data on nucleoside diphosphate kinase (Admiraal et al., 1999).

In a recent crystal structure of UMP/CMP kinase containing AlF_3 as a transition state analog, the observed distances of 2.0 and 2.2 Å between aluminum and the phosphate oxygens suggest a rather associative mechanism (Schlichting & Reinstein, 1997). A putative strongly negatively charged metaphosphate could be stabilized by six positively charged amino acids (Arg42, Arg93, Arg131, Arg137, Arg148, and Lys19) and the Mg^{2+} ion that coordinates the β- and γ-phosphoryl atoms of ATP. A rather associative mechanism is also supported by the crystal structure of UMP/CMP kinase complexed with the bisubstrate inhibitor P^1-(5′-adenosyl)-P^5-(5′-uridyl)-pentaphosphate (Scheffzek et al., 1996).

In cAMP-dependent protein kinase that transfers the γ-phosphate group of ATP to the hydroxy group of a serine residue, a second Mg^{2+} ion is found that is assumed to possess a regulatory function (Madhusudan et al., 1994; Bossemeyer, 1995). It has been suggested that the high number of arginine residues present in UMP/CMP kinase may stabilize a highly charged metaphosphate group in an associative mechanism (Schlichting & Reinstein, 1997; Yan & Tsai, 1999). Such a concentration of positively charged residues is not present in, for example, cAPK (Madhusudan et al., 1994; Mildvan, 1997). Consequently, different mechanisms of phosphoryl transfer could be invoked. On the other hand, this special environment in UMP/CMP kinase may simply be required to allow simultaneous binding of two negatively charged nucleosides.

Despite the structural information on heavy atom coordinates, X-ray data at the given resolution do not reveal the positions of hydrogen atoms and, therefore, no conclusive statement regarding their participation in the reaction mechanism can be made. For example, the existence of a proton on the α-phosphate group of the substrate CMP cannot be ruled out as the local enzymatic environment influences the actual pK_a (Warshel & Åqvist, 1991). For the cAMP-dependent kinase, it was shown by quantum chemical studies that the phosphoryl transfer does not follow a catalytic base mechanism, but instead involves the synchronous shift of the hydroxy-hydrogen to the oxygen atom of the transferred metaphosphate (Hart et al., 1998, 1999; Hutter & Helms, 1999). Assuming a protonated CMP, a similar reaction mechanism could apply to UMP/CMP kinase.

The aim of this study is to elucidate the reaction mechanism of the phosphoryl transfer in UMP/CMP kinase by the means of quantum mechanics, while our results should be of general relevance for the mechanistic understanding of enzymatic phosphoryl transfer in kinases.

Results

Energetic optimization yielded the molecular system shown in Figure 1 with a net neutral charge as the most stable reactant for the phosphoryl transfer. CMP is protonated at P_α and ATP is unprotonated. Attempts to optimize the system with CMP and ATP both being unprotonated, starting from different geometries, resulted in structures that were energetically unfavorable having the γ-phosphate group placed in between the nucleosides in a transition state-like manner. Moving nearby protons from Lys19, Arg42, Arg93, Arg131, Arg137, or Arg148 to CMP again yielded structures that were significantly higher in energy. From the investigated residues, Lys19 is most likely to be deprotonated. However, it appears very unlikely that the proton on CMP originates from one of the positively charged amino acids in the active center. On the other hand, protonation of the terminal phosphate group of ATP resulted in either transition state or product like geometries, indicating the participation of a proton in the reaction mechanism.

The calculated products of the phosphoryl transfer are ADP and protonated CDP (Fig. 2). This product complex is 6.5 kcal mol^{-1} lower in energy than the reactants indicating an exothermic reaction. The actual mechanism of the phosphoryl transfer was visualized by a two-dimensional grid calculation, similarly as previously performed for cAPK (Hutter & Helms, 1999). The potential energy surface was scanned as a function of the distances $d_{[\text{P-OP}]}$ (between the γ-phosphorus of ATP and the nearest oxygen of CMP) and $d_{[\text{PO-H}]}$ (the separation between the oxygen atom on the shifted PO_3-group and the transferred proton). The profile in Figure 3 shows that the apparent reaction path proceeds from the reactants (denoted as circle) over the transition state (denoted as diamond) with an activation barrier of 14.9 kcal mol^{-1} toward the products (denoted as circle). Analysis of the transition state revealed an imaginary frequency of $-1{,}091$ cm^{-1} that is associated with the movement of the shifted proton. Thus, most of the activation energy is spent on moving the proton toward its destination on the γ-phosphate group. The bond formation between P_γ and CMP occurs after passing the transition state while steadily going downhill on the energy surface. Investigation of the bond orders showed that bonding between the P_β-P_γ bridging oxygen and P_γ is not diminished until the transition state is reached.

As observed in crystallographic studies, the side-chain fragments of Arg131, Arg137, and Arg148 show the largest movements during the reaction as they are part of the flexible LID domain in UMP/CMP-kinase (Schlichting & Reinstein, 1997). The side chains of Arg137 and Arg148 are shifted away radially from the active center by about 0.4 Å to make room for the transferred PO_3-group. However, the γ-phosphate group is still coordinated by Arg131, which has its terminal $NHC(NH_2)_2$ fragment rotated about 45°. These structural rearrangements appear to be crucial for the reaction since no product is formed if 10 times stronger constraints are applied to the C_δ atoms of Arg131, Arg137, and Arg148. The side chains of Lys19, Arg42, and Arg93 only show slight movements, and the magnesium ion hardly moves at all which agrees

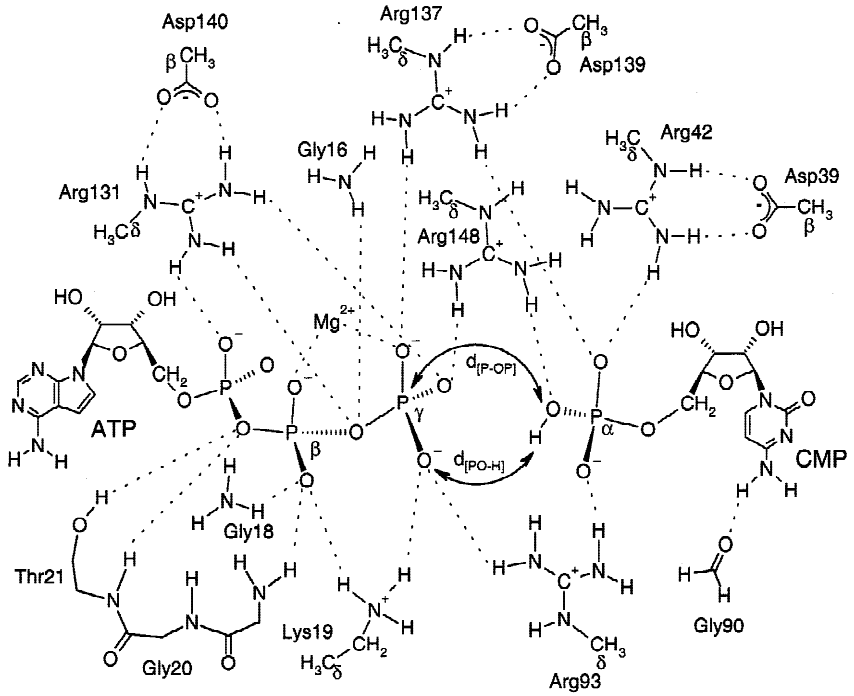

Fig. 1. The quantum mechanical model system derived from the crystal structures (5UKD and 1UKE) of UMP/CMP kinase showing the reactants of the phosphoryl transfer in the forward reaction. For clarity, the eight included water molecules are not shown. Four of them complete the octahedral coordination sphere of the magnesium ion, while the remaining ones form hydrogen bonds to Arg42, Arg93, Asp139, and to the α-phosphate group of CMP.

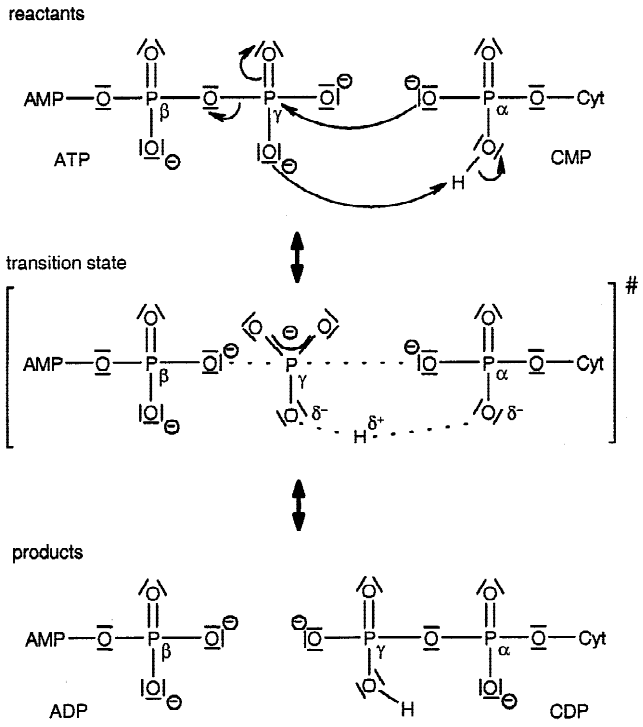

Fig. 2. The concerted phosphoryl transfer mechanism as suggested from the quantum chemical calculations involves the synchronous shift of a proton.

well with the crystallographic findings (Schlichting & Reinstein, 1997).

Alternatively, the molecular systems containing the transition state analogs AlF_3 and AlF_4^- instead of the γ-phosphate group were investigated. We found that if CMP is protonated, both AlF_3 and AlF_4^- adopt nonplanar configurations where aluminum is apically coordinated by the oxygen of the β-phosphate. Conversely, unprotonated CMP leads to almost planar AlF_x geometries, similar to the crystal conformations (Schlichting & Reinstein, 1999).

Important interatomic distances in the computed and crystallographic structures are summarized in Table 1. First of all, the X-ray structure containing AlF_3 (5UKD) and the corresponding computed system (forth column) are in a good agreement. The computed distances between heavy atoms involved in hydrogen bonds are typically longer by 0.05–0.10 Å than their crystallographic counterparts, which is within the experimental error of ~0.1 Å. The strongest deviations occur for Arg137, which rotates about 30° to form a bifurcated hydrogen bond to the phosphate group of CMP. Structural differences between 5UKD and the other computed structures are mostly due to the decreased spacing between P_β of ATP and P_α of CMP, caused by the apical coordination of the aluminum in 5UKD. This compactification leads to a more symmetrical transition state-like structure than our computed transition state geometry and is also observed in crystal structures containing the homologous BeF_2 (Schlichting & Reinstein, 1997). An equally straightforward comparison of the structure containing the bisubstrate inhibitor (1UKE) to either the reactant or the product geometry is hampered by the effect of the additional phosphate group of

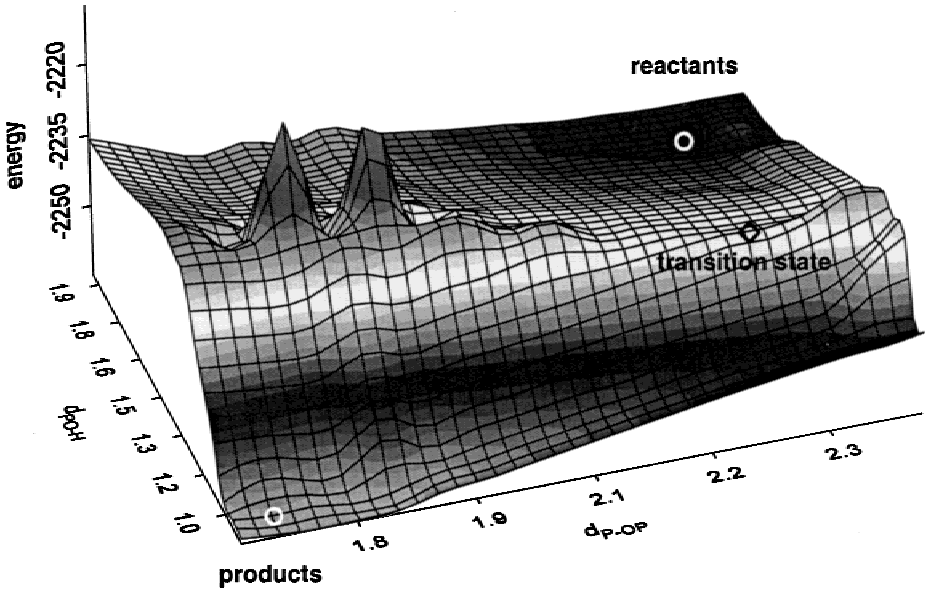

Fig. 3. Two-dimensional energy hypersurface of the phosphoryl transfer (forward reaction). The distances distance $d_{[P\text{-}OP]}$ and $d_{[PO\text{-}H]}$ refer to the corresponding interatomic distances as shown in Figure 1. The energy is given in kcal mol^{-1} and the distances in Å.

P^1-(5′-adenosyl)-P^5-(5′-uridyl)-pentaphosphate that causes strong differences in the region between the P_β of ATP and P_α of CMP. Compared to the reactant as well as the product geometry the residues of the LID domain are shifted outward even more, particularly Arg131, while the position of magnesium is highly conserved. The distance between ATP-P_β and CMP-P_α agrees somewhat better with the value calculated for the product geometry than that of the reactant geometry (Scheffzek et al., 1996).

To gain insight into the charge distribution of the active center during the reaction, a Mulliken population analysis (Mulliken, 1955) was performed for reactant, transition state, and product of the forward reaction. The obtained atomic charges are shown in Table 2 for the transferred PO_3-group in UMP/CMP-kinase and in cAPK (Hutter & Helms, 1999). From the formal description of an associative phosphoryl transfer mechanism, a strong negative charge for the transferred PO_3-group in the transition state has to be

Table 1. *Comparison of important interatomic distances in the computed and in the crystallographic structures between the nonhydrogen atoms marked boldface (in Å)*[a]

	Computed geometries				Crystal structures	
	Reactants	Transition state	Products	AlF_3	5UKD	1UKE
ATP-$\mathbf{P_\beta}$ ↔ CMP-$\mathbf{P_\alpha}$	6.75	6.63	5.96	6.49	6.33	6.36[b]
Lys19**N**Z ↔ P_γ**O**	2.82	2.89	2.90	2.87[c]	2.77[c]	2.69[d]
Lys19**N**Z ↔ P_β**O**	2.80	2.80	2.75	2.76	2.76	2.91
Arg42**N**H1 ↔ CMP-P_α**O**	3.02	3.02	2.96	2.90	2.95	2.79[b]
Arg93**N**H1 ↔ CMP-P_α**O**	2.73	2.71	2.81	2.93	2.81	3.12[b]
Arg93**N**H2 ↔ P_γ**O**	2.88	3.03	3.08	3.01[c]	2.96[c]	3.00[d]
Arg131**N**H1 ↔ ATP-P_α**O**	2.89	2.88	2.76	2.87	2.87	3.02
Arg131**N**H1 ↔ P_β-**O**-P_γ	3.25	3.42	4.29	3.25	3.21	4.74
Arg131**N**H2 ↔ P_γ**O**	2.93	2.95	2.88	3.00[c]	2.90[c]	2.76[d]
Arg137**N**H1 ↔ P_γ**O**	3.17	3.12	3.02	4.97[c]	2.83[c]	3.55[d]
Arg137**N**H2 ↔ CMP-P_α**O**	3.36	3.36	3.42	4.52	3.08	3.71[b]
Arg148**N**H1 ↔ P_γ**O**	3.02	2.98	2.90	2.84[c]	2.50[c]	2.79[d]
Arg148**N**H2 ↔ CMP-P_α**O**	2.96	2.96	3.59	3.14	2.64	4.00

[a] 5UKD and 1UKE refer to the crystal structures containing AlF_3 and the bisubstrate inhibitor P^1-(5′-adenosyl)-P^5-(5′-uridyl)-pentaphosphate, respectively.
[b] CMP-P_α corresponds to P_ϵ of the bisubstrate inhibitor.
[c] P_γ**O** corresponds to Al**F**.
[d] Toward the corresponding P_δ**O** of the bisubstrate inhibitor.

Table 2. *Evolution of the Mulliken charges in the model systems for UMP/CMP-kinase and cAPK during the forward reaction*[a]

Model-system	Fragment	Reactants	Transition state	Product
UMP/CMP-kinase	Transferred PO_3	−0.78	−0.56	−0.23
	Shifted proton	+0.31	+0.38	+0.26
	Transferred PO_3 and H	−0.47	−0.18	+0.03
cAPK	Transferred PO_3	−0.49	−0.27	−0.17
	Shifted proton	+0.31	+0.39	+0.31
	Transferred PO_3 and H	−0.18	0.12	+0.14

[a]Charges in e.

expected. However, we calculate a significant decrease of negative charge of the PO_3-fragment, particularly when taking the simultaneously shifted proton into account. The trends are very similar for both kinase systems, indicating a dissociative-like mechanism. This is also supported by the sum of the distances between the apical oxygen atoms and P_γ in the transition state geometry (4.083 Å).

Discussion

Quantum chemical investigation of the active center of CMP/UMP-kinase containing the reactants ATP and CMP shows that ATP adopts an unprotonated form while CMP is protonated despite the presence of multiple positively charged amino acids. As all attempts failed to yield a suitable reactant geometry with both ATP and CMP being unprotonated, this must be regarded as a strong indication of the participation of a proton in the reaction. It remains, however, unclear where this proton originates from, as all corresponding amino acids in the active site remain protonated throughout the reaction. As suggested by one reviewer, measuring a steady state rate profile of $\log(k_{cat})/K_m$ against pH could provide a useful experimental test of this hypothesis. On the other hand, the relevant pH range is expected around 6–7 and the analysis could be disturbed by surrounding residues in the highly charged protein active site that may have strongly shifted pK_a values. Further studies in our laboratory will investigate the binding energetics of protonated and unprotonated nucleosides by electrostatic continuum calculations similar to a previous study on cAPK (Hünenberger et al., 1999). The uptake of a protonated monophosphate nucleoside from solution is by no means in disagreement with experimental observations.

The structural rearrangements of Arg131, Arg137, and Arg148 were found to be of importance for the course of the reaction. They either belong to the flexible LID domain and/or were shown to undergo the strongest movements in crystal structures of UMP/CMP-kinase with substrates, inhibitors, and transition state analogs bound (Schlichting & Reinstein, 1997). No product at all is formed when they are tightly restrained to their crystallographic positions. On the other hand, Lys19 and Mg^{2+} do not move significantly during the reaction, in agreement with a suggestion by Schlichting and Reinstein (1997) that Lys19 and the magnesium ion provide a structural template for phosphoryl transfer.

Our calculated transition state geometry is less symmetrical than found in the crystal structure containing the transition state analog AlF_3. Comparison with the computed AlF_3 structure shows that apical coordination of aluminum by the terminal phosphate groups leads to a compactification between the nucleosides. The X-ray structure, therefore, would correspond to a transition state with a more associative like character that shows increased density of negative charge on the transferred PO_3-group.

Surprisingly, AlF_3 shows only a low binding affinity despite the apical coordination (Schlichting & Reinstein, 1997), and the number of aluminum coordinating fluorides is pH-dependent in these crystal structures (Schlichting & Reinstein, 1999). AlF_4^- binds at pH 4.5 while AlF_3 is present at pH 8.5. At the lower pH, CMP can be expected to occur protonated in solution while at the higher pH it is likely to be fully deprotonated. In our computational model, we obtain the crystallographically observed planar AlF_x geometry only when CMP is unprotonated, while for the phosphoryl transfer reaction CMP is required to be protonated. Therefore, while being a good structural transition state analog, aluminum fluoride apparently influences the protonation state of the coordinating nucleoside, i.e., CMP. Thus, our results also provide an explanation why planar AlF_3 preferentially binds at pH 8.5. The binding of anionic AlF_4^- should be electrostatically favored in the presence of protonated CMP at pH 4.5. Conversely, this can be regarded as an indirect experimental verification of our prediction regarding the protonation state of CMP.

Our calculated reactant structure (Fig. 1) shows striking similarities to the corresponding complex of ATP and the serine substrate in cAPK. The distance $d_{[P\text{-}OP]}$ between the nearest oxygen of CMP and the γ-phosphorus of ATP (2.442 Å) as well as the separation between ATP and the transferred proton, $d_{[PO\text{-}H]}$ (1.991 Å), closely resemble the values of their counterparts in cAPK (2.496 and 1.992 Å, respectively) (Hutter & Helms, 1999). Furthermore, the energetic profile of the phosphoryl transfer in CMP/UMP-kinase (Fig. 3) and that for cAPK as published earlier (Hutter & Helms, 1999) look very much alike. In both cases, the phosphoryl transfer is accomplished by a simultaneous shift of a hydroxylic proton to one of the oxygens of the transferred PO_3 group. The exothermicity of the reaction is, however, more strongly emphasized in cAPK (-12.2 kcal mol^{-1} compared to -6.5 kcal mol^{-1} here) as can be expected from the difference in pK_a values of the accepting groups (13.4 for serine and 6.5 for CMP), while the activation barrier for the forward reaction ($+14.9$ kcal mol^{-1}) is significantly lower in CMP/UMP-kinase ($+20.7$ kcal mol^{-1} in cAPK). These calculated data are in good agreement with the observed reversibility of the phosphoryl transfer in CMP/UMP-

kinase. The energy difference of 8.4 kcal mol^{-1} is very close to the energy of solvolysis of MgATP, which shows the consistency of our computational models.

The electronic description of the phosphoryl transfer mechanism again shows strong similarities to that of cAPK as the negative charge on the transferred PO_3-group including the shifted proton decreases along the forward reaction.

In summary, the atomic charges and the distance criteria between the apical oxygen atoms and the P_γ-phosphorus in the transition state geometry seem consistent with a dissociative mechanism for phosphoryl transfer in UMP/CMP kinase. However, we find that phosphoryl transfer is accompanied by the synchronous shift of a proton from CMP to the transferred PO_3-group as shown in Figure 2. To our knowledge, this concerted phosphoryl and proton transfer mechanism has not been proposed previously for dinucleoside kinases. The discussion of dissociative vs. associative phosphoryl transfer should be updated to include this novel aspect. A common mechanism has been established for two seemingly unrelated kinases: cAMP-dependent kinase and UMP/CMP kinase. Future work will show whether it can be extended to more members of the kinase family.

Materials and methods

The active site model system used for UMP/CMP-kinase (shown in Fig. 1) contains ATP, CMP, the Mg^{2+}-ion with full coordination shell, and 14 residues thought to be critical for phosphoryl transfer; a total of 236 atoms all of which are treated fully quantum mechanically by the semiempirical AM1 method (Dewar et al., 1985). All calculations were performed using a modified version of the program package VAMP Version 6.5 (Rauhut et al., 1997). The same parameter sets for phosphorus (Dewar & Jie, 1989) and magnesium (Hutter et al., 1998) were employed as in an earlier study on a related protein kinase (Hutter & Helms, 1999).

Initial atomic coordinates of the nonhydrogen atoms in the model system were taken from the X-ray crystallographic structure of UMP/CMP-kinase complexed with ADP, CMP, and the transition state analog AlF_3 (Schlichting & Reinstein, 1997) (5UKD). The crystallographic water molecule numbers 198, 215, 220, and 227 were included to complete the first coordination spheres of the magnesium ion. Furthermore, the water molecules 208, 233, 712, and 880 are present as they are part of the hydrogen bond network in the active site. Not included in the model system are the water molecules 197, 553, and 606 as corresponding analogs are not found in the crystal structure of UMP/CMP-kinase complexed with the bisubstrate P^1-(5′-adenosyl)-P^5-(5′-uridyl)-pentaphosphate (Scheffzek et al., 1996) (1UKE). AlF_3 was replaced by PO_3 forming the γ-phosphate group of ATP. From the residues surrounding the reactants, all five arginine residues are present, each truncated at C_δ. Likewise, the aspartate residues 39, 139, and 140 were capped at C_β. Of Lys19, the terminal C_δ-NH_3 group was included. As Gly16, Gly18, and Gly90 solely are involved in hydrogen bonding to the β-phosphate of ATP and to CMP, they are modeled by ammonia and formaldehyde, respectively, which sufficiently render the electronic properties of a hydrogen bond donor (RR′N—H) and a hydrogen bond acceptor (RR′C=O) within the theoretical framework used. Similar to the truncated side chains, relevant fragments of Thr21 and Gly20 were modeled (see Fig. 1).

Hydrogen atoms were added with initial bond lengths of 1.08 Å assuming the side chains of aspartate, arginine, and lysine to be charged. Together with a protonated phosphate group of CMP (see above), this results in a net neutral charge of the model system.

To emulate the structural effect of the protein backbone, the terminating carbon atoms of the truncated side chains of aspartate, arginine, and lysine acids were harmonically restrained to their crystallographic positions. The backbone nitrogen atoms of Gly16, Gly18, Lys19, Gly20, and Thr21 as well as the carbon atom of Gly90 and the C_α atom of Thr21 were restrained in the same fashion. Compared to a fully rigid fixation, this offers the advantage that stationary points on the energetic hypersurface (minima and transition states) can still be characterized (Clark et al., 1997). Also, the "hardness" of each harmonic potential can be adjusted to suit the environment. For the oxygen atoms of the water molecules, a relatively weak force constant of 1.15 kcal mol^{-1} $Å^{-2}$ was employed. For example, the four water molecules that ligate the magnesium displayed a structural shift of 0.8 Å root-mean-square deviation between the X-ray geometry and the AM1-optimized reactant geometry. This structural rearrangement is caused by the omission of the outer parts of the protein, but is very unlikely to affect the calculated energy barrier of the reaction. Moreover, the magnitude of this structural movement shows the conformational freedom of the water molecules.

For the restrained atoms of the truncated amino acid side chains, a "harder" potential of 230.6 kcal mol^{-1} $Å^{-2}$ was used to account for the effect of the missing protein backbone. For the restrained C_δ atoms of Arg131, Arg137, and Arg148, however, a "softer" potential of 2.31 kcal mol^{-1} $Å^{-2}$ was used as these residues are either part of the flexible LID domain and/or exhibit the highest structural variation between the two considered X-ray structures (Vonrhein et al., 1995; Schlichting & Reinstein, 1997).

Instead of adding further residues to hold the adenosine and cytosine moiety of ATP and CMP in place in a protein-like fashion, constraints were also applied to their N-1, N-9, C-1′, and C-4′ atoms as well as the N-3 atom, respectively. This allowed us to limit the number of atoms to a computable scope.

The Eigenvector Following (EF) algorithm (Baker, 1986) was used throughout all calculations to optimize the model system to a gradient norm below 0.4 kcal mol^{-1} $Å^{-1}$. For the two-dimensional grid calculation, a step size of 0.05 Å was employed.

Acknowledgment

We thank J. Reinstein for a critical reading of the manuscript and helpful discussions and the reviewers for helpful comments.

References

Admiraal SJ, Herschlag D. 1995. Mapping the transition state for ATP hydrolysis: Implications for enzymatic catalysis. *Chem Biol 2*:729–739.

Admiraal SJ, Schneider B, Philippe M, Janin J, Véron M, Deville-Bonne D, Herschlag D. 1999. Nucleophilic activation by positioning in phosphoryl transfer catalyzed by nucleoside diphosphate kinase. *Biochemistry 38*:4701–4711.

Åqvist J, Fothergill M, Warshel A. 1993. Computer simulation of the CO_2/HCO_3^- interconversion step in human carbonic anhydrase I. *J Am Chem Soc 115*:631–635.

Baker J. 1986. An algorithm for the localization of transition-states. *J Comput Chem 7*:385–395.

Bossemeyer D. 1995. Protein kinases—Structure and function. *FEBS Lett 369*:57–61.

Clark T, Gedeck P, Lanig H, Schürer G. 1997. Semiempirical MO—Calculations on enzyme reaction mechanisms. In: Banci L, Comba P, eds. *Molecular modelling and dynamics of bioinorganic systems*, NATO ASI series 3, Vol. 41. Dordrecht: Kluwer Academic Publishers. pp 307–318.

Dewar MJS, Jie CX. 1989. AM1 parameters for phosphorous. *J Mol Struct (THEOCHEM) 187*:1–13.

Dewar MJS, Zoebisch EG, Healy EF, Stewart JJP. 1985. The development and use of quantum-mechanical molecular-model: 76. AM1—A new general-purpose quantum-mechanical molecular-model. *J Am Chem Soc 107*:3902–3909.

Gao J. 1995. Methods and applications of combined quantum mechanical and molecular mechanical potentials. In: Lipkowitz KB, Boyd DB, eds. *Reviews in computational chemistry*. Vol. 7. New York: VCH. pp 119–185.

Hart JC, Hillier IH, Burton NA, Sheppard DW. 1998. An alternative role for the conserved Asp residue in phosphoryl transfer reactions. *J Am Chem Soc 120*:13535–13536.

Hart JC, Sheppard DW, Hillier IH, Burton NA. 1999. What is the mechanism of phosphoryl transfer in protein kinases? A hybrid quantum mechanical/molecular mechanical study. *Chem Commun* 79–80.

Hu C-H, Brinck T. 1999. Theoretical studies of the hydrolysis of the methyl phosphate anion. *J Phys Chem A 103*:5379–5386.

Hünenberger P, Helms V, Narayana N, Taylor SS. 1999. Determinants of ligand binding to cAMP-dependent protein kinase. *Biochemistry 38*:2358–2366.

Hutter MC, Helms V. 1999. Influence of key residues on the reaction mechanism of the cAMP-dependent protein kinase. *Protein Sci 8*:2728–2733.

Hutter MC, Reimers JR, Hush NS. 1998. Modeling the bacterial photosynthetic reaction center. 1. Magnesium parameters for the semiempirical AM1 method developed using a genetic algorithm. *J Phys Chem B 102*:8080–8090.

Madhusudan, Trafny EA, Xuong N-H, Adams JA, Ten Eyck LF, Taylor SS, Sowadski JM. 1994. cAMP-dependent protein kinase: Crystallographic insights into substrate recognition and phosphotransfer. *Protein Sci 3*:176–187.

Merz KM, Dewar MJS, Hoffmann R. 1989. Mode of action of carbonic anhydrase. *J Am Chem Soc 111*:5636–5649.

Mildvan AS. 1997. Mechanism of signaling and related enzymes. *Proteins 29*:401–416.

Mulliken RS. 1955. Electronic population analysis on LCAO-MO molecular wave functions I. *J Chem Phys 23*:1833–1846.

Rauhut G, Alex A, Chandrasekhar J, Steinke T, Sauer W, Beck B, Hutter M, Gedeck P, Clark T. 1997. VAMP Version 6.5. Erlangen: Oxford Molecular.

Scheffzek K, Kliche W, Wiesmüller L, Reinstein J. 1996. Crystal structure of the complex UMP/CMP kinase from *Dictyostelium discoideum* and the bisubstrate inhibitor P1-(adenosine 5′)-P5-(uridine 5′)-pentaphosphate (UP5A) and Mg2+ at 2.2 Å: Implications for water-mediated specificity. *Biochemistry 35*:9716–9727.

Schlichting I, Reinstein J. 1997. Structures of active conformations of UMP kinase from *Dictyostelium discoideum* suggest phosphoryl transfer is associative. *Biochemistry 36*:9290–9296.

Schlichting I, Reinstein J. 1999. pH influences fluoride coordination of the AlFx phosphoryl transfer transition state analog. *Nat Struct Biol 6*:721–723.

Schweins T, Geyer M, Kalbitzer HR, Wittinghofer A, Warshel A. 1996. Linear free energy realtionships in the intrinsic and GTPase activating protein-stimulated guanosine 5′-triphosphate hydrolysis of p21 ras. *Biochemistry 35*:142250-14231.

Schweins T, Langen R, Warshel A. 1994. Why have mutagenesis studies not located the general base in ras p21. *Nat Struct Biol 1*:476–484.

Vonrhein C, Schlauderer GJ, Schulz GE. 1995. Movie of the structural changes during a catalytic cycle of nucleoside monophosphate kinases. *Structure 3*:483–490.

Warshel A, Åqvist J. 1991. Electrostatic energy and macromolecular function. *Annu Rev Biophys Biophys Chem 20*:267–298.

Yan H, Tsai M-D. 1999. Nucleoside monophosphate kinases: Structure, mechanism, and substrate specificity. In: Purich DL, ed. *Mechanism of enzyme action, Part A, Advances in enzymology and related areas of molecular biology*. Vol. 73. Chichester: John Wiley & Sons, Inc. pp 103–134.